

Convolutional Recurrent Neural Networks for Glucose Prediction

Kezhi Li, John Daniels, Chengyuan Liu, Pau Herrero, Pantelis Georgiou

Department of Electronic and Electrical Engineering, Imperial College London, London SW7 2AZ, UK

Abstract—Control of blood glucose is essential for diabetes management. Current digital therapeutic approaches for subjects with Type 1 diabetes mellitus (T1DM) such as the artificial pancreas and insulin bolus calculators leverage machine learning techniques for predicting subcutaneous glucose for improved control. Deep learning has recently been applied in healthcare and medical research to achieve state-of-the-art results in a range of tasks including disease diagnosis, and patient state prediction among others. In this work, we present a deep learning model that is capable of forecasting glucose levels with leading accuracy for simulated patient cases (RMSE = 9.38 ± 0.71 [mg/dL] over a 30-minute horizon, RMSE = 18.87 ± 2.25 [mg/dL] over a 60-minute horizon) and real patient cases (RMSE = 21.07 ± 2.35 [mg/dL] for 30-minute, RMSE = $33.27 \pm 4.79\%$ for 60-minute). In addition, the model provides competitive performance in providing effective prediction horizon (PH_{eff}) with minimal time lag both in a simulated patient dataset ($PH_{eff} = 29.0 \pm 0.7$ for 30-min and $PH_{eff} = 49.8 \pm 2.9$ for 60-min) and in a real patient dataset ($PH_{eff} = 19.3 \pm 3.1$ for 30-min and $PH_{eff} = 29.3 \pm 9.4$ for 60-min). This approach is evaluated on a dataset of 10 simulated cases generated from the UVA/Padova simulator and a clinical dataset of 10 real cases each containing glucose readings, insulin bolus, and meal (carbohydrate) data. Performance of the recurrent convolutional neural network is benchmarked against four algorithms. The proposed algorithm is implemented on an Android mobile phone, with an execution time of 6ms on a phone compared to an execution time of 780ms on a laptop.

Index Terms—Type 1 diabetes, continuous glucose monitor (CGM), glucose prediction, deep learning, long short term memory (LSTM).

I. INTRODUCTION

Diabetes is a chronic illness characterised by the absence of glucose homeostasis. A healthy pancreas dynamically controls the release of insulin and glucagon hormones through the α -cells and β -cells respectively, in order to maintain euglycaemia [1]. In Type 1 diabetes, an autoimmune disease, the β -cells are compromised and therefore suffer from impaired production of insulin. This leads to periods of hyperglycaemia (persistent blood glucose (BG) concentration $> 180\text{mg/dL}$) and hypoglycaemia (BG concentration $< 70\text{mg/dL}$) [2], [3]. Insulin therapy is needed to maintain BG levels in the advised target range [4].

The standard approach to diabetes management requires people actively taking BG measurements a handful of times throughout the day with a finger prick test - self monitoring of blood glucose. The recent development and uptake of continuous glucose monitoring (CGM) devices allow for improved sampling (5 minutes) of glucose measurements [5]. This approach has proven to be effective in controlling BG and thus improving the outcome of subjects in clinical trials

[6]. Further improvement of glucose control can be realised through prediction, which allows users to take actions ahead of time in order to minimise the occurrence of adverse glycaemic events. The challenges lie in multiple factors that influence glucose variability, such as insulin variability, ingested meals, stress and other physical activities [7]. In addition, individual glycaemic responses are conditioned by high subject variability [4], [8], leading to different responses between individuals under the same conditions.

Machine learning (ML) allows intelligent systems to build appropriate models by learning and extracting patterns in data. The models discover mappings from the representation of input data to the output. Performances of traditional machine learning algorithms such as logistic regression, k-nearest neighbours [9], or support vector regression [10] heavily rely on the representation of the data they are given. Typically, the features - information the representation comprises - are engineered with prior knowledge and statistical features (mean, variance) [11], principal component analysis (PCA) [12] or linear discriminant analysis [13]. Artificial neural networks (ANN) are also investigated widely in diabetes management [14]–[18]. One advantage of ANN is that, normally no hand-craft feature finding is required. However, ANN in the literature are mostly implemented fewer than 3 layers, hence its learning capacity is limited due to the model complexity. Deep learning, which incorporates multi-layer neural networks, has led to significant progresses in computer vision [19], diseases diagnosis [20], and healthcare [21], [22]. Deep learning shows superior performance to traditional ML techniques due to this ability to automatically learn features with higher complexity and representations [23]–[26]. As a result, it encodes features that might not be previously known to researchers.

In this paper, we propose a deep learning algorithm for glucose prediction using a multi-layer convolutional recurrent neural network (CRNN) architecture. The model is primarily trained on data comprising CGM, carbohydrate and insulin data. After preprocessing, the time-aligned multi-dimensional time series data of BG, carbohydrate and insulin (other factors also can be considered) are fed to CRNN for training. The architecture of the CRNN is composed of three parts: a multi-layer convolutional neural network that extracts the data features using convolution and pooling, followed by a recurrent neural network (RNN) layer with long short term memory (LSTM) cells and fully-connected layers. The model is trained end-to-end. The convolutional layer comprises a 1D Gaussian kernel filter to perform the temporal convolution, and pooling layers are used for reducing the feature set. A variant of LSTM

model is leveraged since LSTM shows good performances in predicting time series with long time dependencies [27]. The final output is a regression output by fully connected layers. The CRNN model is realized using the open-source software library Tensorflow [28], and it can be easily implemented to portable devices with its simplified version Tensorflow Lite. The performance of the proposed method is evaluated on datasets of simulated cases as well as clinical cases of T1DM subjects, and compared against benchmark algorithms including support vector regression (SVR) [10], the latent variable model (LVX) [29], the autoregressive model (ARX) [30], and neural network for predicting glucose algorithm (NNPG) [14]. The results show the competitive performance of the method.

As far as we know, the proposed method is a pioneering work in glucose forecast implementing deep neural networks that incorporates the merits of both CNN and RNN, and we modify them to suit the task of glucose prediction. It achieves competitive performances in terms of forecasting accuracy comparing to benchmark methods, with superior performances in terms of RMSE. It applies multi-layer NN in smart phones with applications in diabetes management. The paper is organized as follows. Section II briefly introduces the properties of the glucose data. Section III addresses the method and architecture of the proposed convolutional recurrent neural network. The performance of the proposed method is evaluated and discussed in Section IV. Section V discusses important details of the method. Finally Section VI summarizes the paper.

II. DATA ACQUISITION AND SETTING

A. Data Acquisition

The data used in this paper include two datasets, *in-silico* data and clinical data. *In-silico* data consisting of 10 adult T1DM subjects was generated using the UVA/Padova T1D, which is a simulator for glucose level simulation approved by the Food and Drug Administration (FDA) [31]. In this work, we used a modified version of the simulator which includes such variability. In particular, the variability on meal composition, insulin absorption, carbohydrate estimation and absorption, and insulin variability were included. In addition, a simple model of physical exercise was also used. Details about how the simulator was modified can be found in [32].

Clinical data was obtained from a clinical study at Imperial College Healthcare NHS Trust St. Marys Hospital, London (UK) consisting of multiple phases evaluating the benefits of an advanced insulin bolus calculator for T1D subjects [33]. The dataset in consideration was collected from a 6-month period involving 10 adult subjects with T1D. The information included in the dataset comprises glucose, meal, insulin, and associated time stamps. In building the dataset, we mainly consider CGM and self-reported data such as insulin boluses, meals, and exercise similar to the *in-silico* dataset. Before that, we exclude participants whose data exhibited large gaps (corresponding to weeks of missing data), insufficient reports of exercise over the 6-month period, and extensive errors in sensor readings.

The CRNN model can be applied to datasets where other inputs are available, such as self-reports of exercise, stress

and alcohol consumption. We believe that these information are useful and will increase the forecast accuracy in some cases. But in this section we only consider CGM data recorded every 5 minutes, meal data indicating meal time and amount of carbohydrates, as well as insulin data with each bolus quantity and the associated time as input in the model.

B. Data Setting

The *in silico* data considered in this section is generated via UVA/Padova T1D. This simulator serves as robust and validated framework for generating simulated cases. The cohort of T1D cases generated can be configured with varying meal and insulin information such that each case sufficiently differs. We generate a dataset of 10 unique adult cases and each has 360 days of data for each case. There are 3 meals per day. Insulin entries vary in each day, from 1 to 5. The insulin entry can be with a meal (meal and insulin at almost the same time), or without a meal (correction bolus). A simple exercise model is considered at certain points, which occur occasionally at any time except for nights. The training data accounts for 50% of the dataset, and the testing set is the rest of data.

The clinical data was collected from T1DM subjects in a 6 month clinical trial. The CGM data was measured using Dexcom G4 Platinum CGM sensors, with measurements received every 5 minutes. The CGM sensors were inserted from the first day of the study, and calibrated according to the manufacturer instructions. Other information available in the dataset such as meal, insulin, exercises was logged by the diabetic subjects themselves. Though the selected data has good quality, many periods of missing data, bad points or unexpected fluctuations exist. Similar to the *in silico* experiment, each subject's clinical data is halved for training and testing data.

III. METHODS

After introducing the data acquisition and setting, the method is explained explicitly. The approach consists of several components: preprocessing, feature extraction using CNN, time series prediction using LSTM and a signal converter. The architecture of the proposed CRNN is shown in Fig. 1. In the diagram, the input of the algorithm is time series of glycaemic data from CGM, carbohydrate and insulin information (time and amount); other related information are optional (exercises, alcohol, stress, etc.). The output of preprocessing is cleaned as time-aligned glycaemic, carbohydrate and insulin data, which are then fed to the CNN. The output of CNN serves as the input of RNN, which is a multi-dimensional time series data, representing the concatenation of features of the original signals. The output of the RNN is the predictive BG level 30-min (or 60-min) later, while hidden states are inherited and updated continuously internally inside of the RNN component. The model is trained end-to-end. We evaluate the models with 30 and 60-min prediction horizon (PH) because it is widely used in glucose prediction software, and is easier to compare results with other works [10], [14], [16], [29], [34], [35]. We proceed with an explanation data pipeline and components of the model architecture.

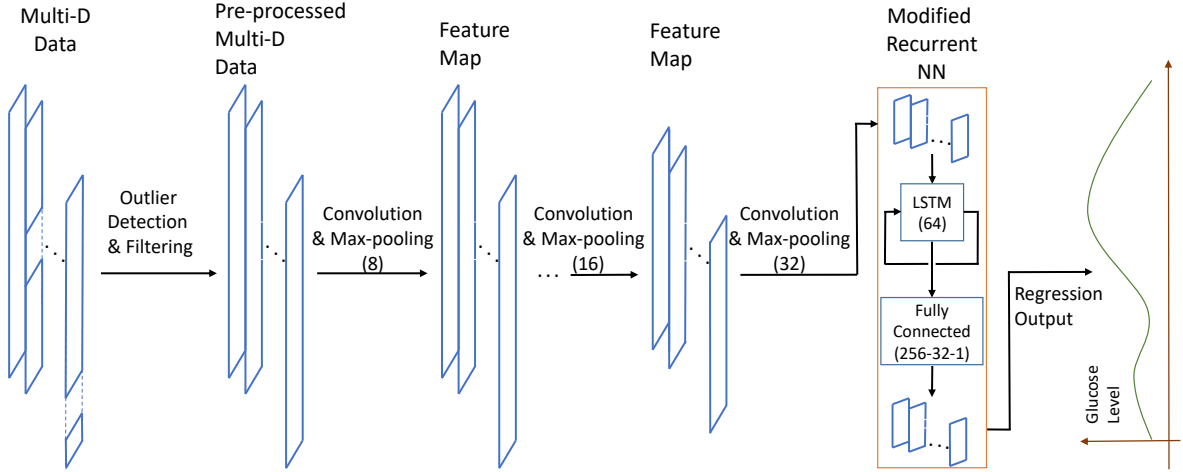


Fig. 1. The architecture of the proposed convolutional recurrent neural network for BG prediction. The data at the left is the concatenated time series data including glucose level, carbohydrate, insulin and other factors. After outlier filtering, the multi-dimensional data can be sent to the multi-layer convolutional component. Then the resultant time series is sent to the modified recurrent neural network component presented in a red frame, which includes LSTM cells and dense fully connected layer. Finally, the resultant is converted back from “change of the glucose value” to “absolute glucose value”. The output is the future glucose values of PH (eg. PH = 30 mins).

A. Outlier Detection and Filtering

The main purpose of the preprocessing component is to clean the data, filter the unusual points and make it suitable as the input to the neural network. Besides the normal steps including time stamp alignment and normalization, the most important operation to improve the data quality is the outlier detection, interpolation/extrapolation and filtering, in particular for clinical data. Because in clinical data, there are many missing or outlier data points due to errors in calibration, measurements, and/or mistakes in data collection and transmission. Here, several methods can be used to handle these scenarios [36]. They include dimension reduction model to project data into lower dimensions [37], proximity-based model to determine the data by cluster or density [38], and probabilistic stochastic filters [39] to rule out outliers.

For some cases when the data fluctuates with high frequency, 1D Gaussian kernel filter can be implemented on the glucose time series. A smoothed continuous time series of glycaemic data can be obtained, along with the time-aligned carbohydrate and insulin information. In this paper, for *in silico* data we do not use filters because the dataset is already clean. For clinical data used in this paper, we use the Gaussian filter. The 3-dimensional time series that covers the last 2 hours before the current time is sent to the neural network as input. A sliding window of size 24 is determined to train the model. Because during the experiments we find that 24 is an optimal setting considering the tradeoff between the prediction accuracy and the computation complexity. In [14] the NNPG algorithm uses a similar window size of 20.

B. A Multi-layer Convolutional Network

The filtered time series signal goes through the multi-layer convolutions, which transform the input data into a set of feature vectors. The convolution operation follows the

temporal convolution definition in which

$$z[m] = \sum_{i=-l}^l x[i] \cdot \delta[m-i], \quad (1)$$

where x represents the input signal, δ denotes the kernel, z is the result of the convolution, and m is the result’s index. Specifically in the first layer, x ’ length is the sliding window size of 24, kernel δ has a size of 8. The dimension of data in each layer can be referred to the Appendix. The input signal can be fed using a sliding window setting. The windows can be overlapped or non-overlapped, determined by the allowed CNN size and computations. The CNN automatically learns the associated weights and recognises particular patterns and features in the input signal that can best represent the data for future time steps. It is illustrated in Fig. 2.

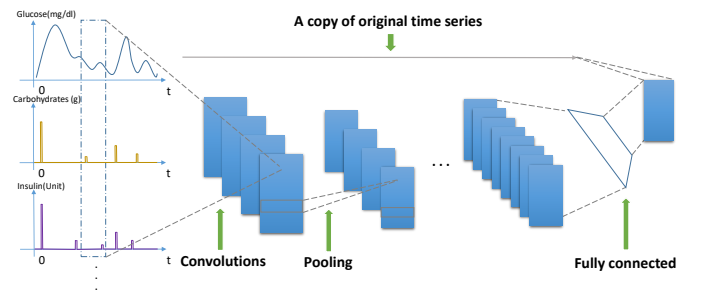


Fig. 2. An illustration of the proposed CNN architecture. The multi-dimensional aligned time series data are concatenated, and then sent to a multi-layer CNN composed of convolutional layers and pooling layers. Finally, after going through a fully connected layer, the final output is the summation of the model output and a copy of the original CGM time series.

The proposed CNN consists of 3 convolutional layers, with max pooling applied to down-sample the feature map obtained from the previous convolutional layer. It is common to periodically insert a pooling layer in-between successive convolutional layers to progressively reduce the size of the

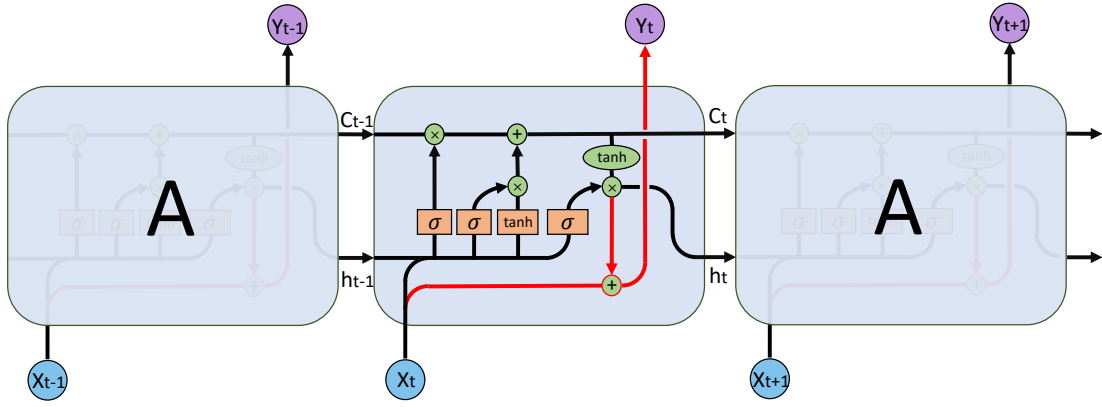


Fig. 3. An illustration of the proposed modified recurrent neural network in the inference. It originates from the conventional LSTM cell, including an input gate, an output gate and a forget gate. The difference lies in the output part, which indicates in red colour in the figure. The output of h_t is still the internal parameter which is transmitted to the next cell. However, the output value signal is y_t instead of h_t . It is because in the training process, the target of RNN is the change of the glucose value between current time and 30 mins later. Thus the predictive glucose level after 30 mins should be the inference value plus the current glucose value.

representation, as well as the computation. It also guards against the problem of overfitting. For instance, if the accepted size is $L1 \times D1$, and the down-sampled parameters are spatial extent F and stride S , and it results in a max-pooling vector Y of size $L2 \times D2$ where

$$L2 = (L1 - F)/S + 1; D2 = D1; Y_i = \max(y_i^*) \quad (2)$$

where y_i^* is the vectors after being down-sampled, Y_i is the feature map and $\max()$ is the operator that computes the maximum value. During the training process, the CNN is trained by back-propagation and the stochastic gradient descent method. The initial weights of the network are set randomly, and the mean-absolute-error is set as the cost function to be minimised in the training. Partial derivatives of the error in terms of the weights w_i and bias b_i are computed, and the associated w_i and b_i are updated accordingly. The last convolutional layer feeds directly into the recurrent layer that makes up the next component in the architecture.

C. A Modified Recurrent Layer

An LSTM network comprised of 64 LSTM cells is adopted as recurrent layers [40]. Each LSTM cell consists of an input gate, an output gate and a forget gate. Each of the three gates can be thought of as a neuron, and each gate achieves a particular function in the cell. The LSTM network is good at building predictive models for time series and sequential data [41]. These cells retain previous data patterns over arbitrary time intervals, thus the internal ‘‘memory’’ can predict the future output according to the previous states. Its memory can be updated simultaneously when new data are fed to the model.

The output of the CNN, a multi-dimensional time series, is connected to the LSTM network. We generated an RNN with 1 hidden layer, consisting of a wide LSTM layer consisting of 64 cells. A dropout applied after the LSTM layer. Dropout refers to ignoring neurons randomly during the training phase. It has been verified that in many cases that dropout can effectively avoid overfitting problems and improve the generalisation [42].

The main difference between a normal LSTM and the proposed LSTM is that the proposed model has a transform and a recovery step. They modify BG values before and after the conventional LSTM. In training phase, instead of BG values directly, we use the changes of BG between the current BG $x(t)$ and the future BG $x(t+6)$ as target labels. It is called the transform step. The input sliding window matrices are multi-dimensional time series (including BG values, meal, insulin). After the model has been trained, the inference output is the change of BG $\Delta x(t)$ between $x(t)$ and $x(t+6)$. Thus the prediction of BG at time $t+6$ can be calculated as $x(t+6) = x(t) + \Delta x(t)$. This is called the recovery step.

Specifically, a modified LSTM estimates the conditional probability $p(y_1, \dots, y_{T'} | x_1, \dots, x_T)$ given a sequence of data, where x_1, \dots, x_T denotes the input sequence and $y_1, \dots, y_{T'}$ is the corresponding output sequence, with size T and T' respectively. If x_t, h_t, c_t are used to denote the input vector, output vector and memory cell vector respectively; W, U , and b are the parameter matrices/vectors that can be learned in the network. f_t, i_t , and o_t denote the forget gate, input gate, and output gate vectors. Then mathematical form of the update process can be explicitly written as

$$\begin{aligned} f_t &= \sigma_g(W_f x_t + U_f h_{t-1} + b_f) & i_t &= \sigma_g(W_i x_t + U_i h_{t-1} + b_i) \\ o_t &= \sigma_g(W_o x_t + U_o h_{t-1} + b_o) & g_t &= \sigma_t(W_g x_t + U_g h_{t-1} + b_g) \\ c_t &= f_t \circ c_{t-1} + i_t \circ \sigma_t(g_t) & h_t &= o_t \circ \sigma_t(c_t), \\ y_t &= o_t \circ \sigma_t(c_t) + x_t, \end{aligned} \quad (3)$$

where $\sigma_g, \sigma_t, \circ$ is the sigmoid function, hyperbolic tangent and entrywise product, respectively. In (3), the 1st to 5th equations are the same to the equations of normal LSTM. However the last 2 equations of h_t and y_t are modified accordingly. It has been shown in Fig. 3, where the difference between the proposed modified LSTM and the normal LSTM is indicated in red. The output of the LSTM cell is not h_t , but y_t in inference. The h_t is used as an internal hidden state that goes to the next time step. The output y_t is calculated from h_t plus the original input x_t . That is because the output (and targets)

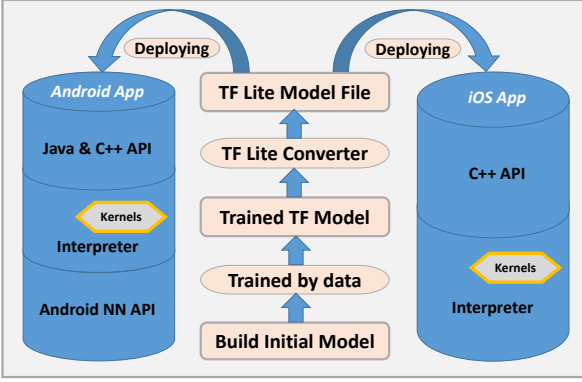


Fig. 4. A flow diagram explains the procedure to implement deep learning models as Tensorflow Lite files to portable devices. In the figure, yellow square frames denote the models or files obtained after each operation, and yellow elliptical frames denote the associated operations applied. After TF Lite model files are created, they can be deployed in Android or iOS app with slightly different settings as shown in the cylinders.

of the neural network is the change of the BG level. The value of the predictive glucose level needs to be recovered from the glucose change by adding the baseline glucose value.

Finally, the last layer of RNN feeds a multi-layer fully connected network, which consists of 2 hidden layers (256 neurons and 32 neurons) and an output layer (a single neuron) with the glucose change as output. The fully connected layer produces the output with an activation function

$$Z_i = act\left(\sum_{i=1}^N Y_i w_i + b_i\right), \quad (4)$$

where Z_i is the multi-dimensional output, $act()$ is an activation function, w_i and b_i are weights of the fully connected network. Particularly, $act()$ can be chosen from a set of activation functions such as sigmoid function $act(a) = 1/(1 + e^{-a})$, rectifier $act(a) = \log(1 + \exp(a))$ or simple linearly $act(a) = a$. In this paper we choose the linear function $act(a) = a$ as the activation function for its simplicity. In the training, a gradient descent optimisation is used. The mean absolute error between the target and the predictive value is being minimised. The optimiser we use is *RMSprop*, because it is a good choice for recurrent neural networks. It usually maintains a moving (discounted) average of the square of gradients [43], and divides gradient by the root of this average.

D. Software and Hardware

After the model has successfully undergone training and validation, we implement our algorithm on mobile phones through Tensorflow Lite due to its efficiency running on portable devices. The model is converted to a Lite model file and installed on an Android or iOS system. It needs the associated application programming interface (API) and interpreter to carry out the inference. Fig. 4 shows how the Tensorflow Lite model file [28] is wrapped and loaded in a mobile-friendly format.

CGM sensors were used to collect data. We utilize computers equipped with graphics processing unit (GPU) to carry out the training and inference processes. In practice an Intel

i7-7700K CPU with 4.20 GHz, 32.0 GB memory with GPU NVIDIA GeForce GTX 1080 Ti were used in the experiments. The program was written in Python 3.6, using CUDA 9.0 to perform the parallel computing. Tensorflow architecture was implemented, because its compatibility and merits for large-scale distributed training and inference.

IV. RESULTS

In this section we test the proposed CRNN algorithm for glucose level forecasting using a *in silico* dataset and a clinical dataset. The performance of the proposed algorithm is contrasted with that of four baseline methods: NNPG, SVR, LVX and ARX (3rd order). The results are compared with the same input data after the same pre-processing. The performance of the methods are compared based on the accuracy over 30- and 60-minute prediction horizon. In addition, we evaluate the time lag of the prediction. Different algorithms were tested on the *in silico* data generated in a way described previously. The parameters involved in these algorithms are tuned carefully for optimal result. In SVR, the SVR function in Python is applied with the optimal parameters ($C = 1e2, \gamma = 0.01, cache_size = 1000$). The LVX method is applied based on the MATLAB code provided in [29], the optimal predictor length and the number of LVs are $J_x = 4$ and $N_{LV} = 4$ respectively. This represents 20-minute historical data of glucose measurement, insulin and meal information being used for prediction. The 3rd order ARX model is optimized by MATLAB function $arx()$ for every specific subject.

A. Criteria for Assessment

Several criteria are used to test the performance of the proposed algorithm. The root-mean-square error (RMSE) and mean absolute relative difference (MARD) between the predicted and reference glucose readings serve as the primary indicators to evaluate the accuracy.

$$RMSE = \sqrt{\frac{1}{N} \sum_{k=1}^N (y(k) - \hat{y}(k|k - PH))^2}, \quad (5)$$

where $\hat{y}(k|k - PH)$ denotes the prediction results provided the historical data and y denotes the reference glucose measurement, and N refers to the data size.

$$MARD = \frac{1}{N} \sum_{k=1}^N \frac{|\hat{y}_k(k|k - PH) - y(k)|}{y(k)}. \quad (6)$$

The RMSE and MARD provide an overall indication of the predictive performance. As mentioned earlier, the benefit of glucose prediction is avoiding adverse glycaemic events. In the clinical context, these metrics are limited in the insight they provide. Additional metrics are needed to assess the proposed algorithm in the following perspective:

- Capability of the forecasting algorithm in differentiating between adverse glycaemic events and non-adverse glycaemic events.
- Time delay in the predicted glucose readings and reference values to evaluate the response time provided to deal with the potential adverse glycaemic event.

The Matthews Correlation Coefficient (MCC) is used to evaluate the performance of the algorithms for detecting either adverse glycaemic event (hypoglycaemia or hyperglycaemia).

$$MCC = \frac{(TP \times TN) - (FP \times FN)}{\sqrt{(TP+FP)(TP+FN)(TN+FP)(TN+FN)}}, \quad (7)$$

where TP , FP , FN , TN stand for true positive, false positive, false negative, and true negative respectively. Here, positive indicates a hypoglycaemia (< 70 mg/dL)/hyperglycaemia (> 180 mg/dL) event in the next or previous 30 or 60 minutes, and true means that the classification is correct. We consider a true adverse event to have occurred when either scenario persists in the CGM data for at least 20 minutes [44]. In addition, we consider an event a True Positive when the predicted event is at most 10 minutes (PH+2 timesteps ahead) leading or within 25 minutes of the prediction horizon lapsing (1 timestep for PH = 30 min, and 7 timesteps for PH = 60 min) the reference event. A standard confusion matrix typically includes the Accuracy as opposed to Matthews Correlation Coefficient (MCC). This modification addresses the imbalance in classes inherent in this situation - non-adverse events far outweigh adverse events.

The effective prediction horizon is defined as the prediction horizon, taking into account delays due to the responsiveness of the algorithm for a predicted value relative to its reference value. Cross correlation of the predicted and actual readings is employed in performing a time delay analysis of the proposed algorithm to determine the effective prediction horizon.

$$\begin{aligned} PH_{eff} &= PH - \tau_{delay} \\ &= PH - \arg \max_{\tau} (\hat{y}_k(k|k - PH) \star y(k)). \end{aligned} \quad (8)$$

A singular quantitative metric is not sufficient in evaluating performance of the proposed algorithm. Consequently, the set of metrics collectively give a comprehensive description of the quality of the prediction algorithm performance. p -values are calculated for other algorithms comparing to the proposed algorithm in terms of smaller RMSE, MARD or longer PH_{eff} . A Shapiro-Wilk Test is used to ascertain the normality of the results before performing a paired t-test to derive the p -values. Across all results, the tests show the null hypothesis (samples drawn from a Gaussian distribution) cannot be rejected.

B. In Silico Data

The results of RMSE, MARD and forecasting of adverse glycaemic events are summarized in the Table I. In the Table we compare the predictive error of the algorithms to measure the accuracy of the algorithms. The CRNN algorithm exhibits the best overall RMSE and MARD for the 10 simulated cases at short(30) and long term(60) predictions. The results in Table I are statistically significant relative to each algorithm. This observation is also evident in both the hyperglycaemia and hypoglycaemia region. In the hyperglycaemia region the CRNN shows a statistically significant improvement in the glucose prediction over most other algorithms, with the exception of LVX. CRNN reports a statistically significant improvement in

TABLE I
RMSE AND MARD COMPARISON OF DIFFERENT PREDICTION METHODS FOR 10 VIRTUAL ADULT DIABETIC SUBJECTS

PH	Metric	CRNN	NNPG	SVR	LVX	ARX
		Overall				
30	RMSE (mg/dL)	9.38 ±0.71	12.91 [‡] ±1.19	12.48 [‡] ±1.94	11.32 [†] ±1.34	13.27 [‡] ±1.19
	MARD (%)	5.50 ±0.62	7.05 [‡] ±0.94	6.40 ±1.36	6.59 [†] ±0.80	7.46 [‡] ±1.02
	Hyperglycaemia					
	MCC	0.84 ±0.05	0.83 ±0.04	0.84 ±0.04	0.83 ±0.04	0.81 ±0.05
	Hypoglycaemia					
	MCC	0.79 ±0.15	0.64 ±0.20	0.79 ±0.10	0.83 ±0.06	0.78 ±0.10
	Effective Prediction Horizon					
Time (min)	29.0 ±0.7	20.8 [‡] ±1.8	23.3 [‡] ±1.6	27.5 [†] ±1.3	20.5 [‡] ±1.7	
60	Overall					
	RMSE (mg/dL)	18.87 ±2.25	24.24 [‡] ±3.01	23.46 [‡] ±3.33	22.42 [†] ±2.74	25.73 [‡] ±3.24
	MARD (%)	9.16 ±1.16	13.70 [‡] ±1.88	10.83 ±1.48	12.20 [‡] ±1.82	13.75 [‡] ±2.45
	Hyperglycaemia					
	MCC	0.82 ±0.05	0.79 ±0.06	0.78 ±0.07	0.86 ±0.04	0.64 ±0.05
	Hypoglycaemia					
	MCC	0.80 ±0.14	0.38 ±0.39	0.79 ±0.10	0.80 ±0.07	0.72 ±0.12
Effective Prediction Horizon						
Time (min)	49.8 ±2.9	31.0 [‡] ±4.7	32.6 [‡] ±4.1	44.2 [‡] ±2.7	19.8 [‡] ±2.7	

* p -value ≤ 0.05 † p -value ≤ 0.01 ‡ p -value ≤ 0.005

effective prediction time (+1.5min for 30-min and +5.6min for 60-min) over LVX, and it is better than the rest thus giving the user more time to take action. On the whole CRNN can be evaluated as the best algorithm. The CRNN model also reports relatively low standard deviations from which we infer a benefit in building individualized models.

An illustration of a comparison of various algorithms for 30-minute shown in Fig. 5 for a virtual adult 4. As seen in Fig. 5, CRNN exhibits the best responsiveness as the predictive curve responds rapidly towards the sharp glycaemic uptrend. The algorithm learns representations that appropriately account for both sharp slopes and gradual increments in the glycaemic curve. Consequently, at a glycaemic peak, CRNN yields a predictive curve with even higher slope to compensate the time lag aiming at reducing the gap between the prediction and real measurements. This feature helps CRNN to decrease the RMSE and MARD as well as maximising the effective prediction horizon.

C. Clinical Data

As mentioned in the previous section, the data obtained in the clinical trial exhibits missing data, and erroneous data. This results in non-physiological discontinuities that would affect the training process. To mitigate these occurrences, the data is processed with interpolations/extrapolations for gaps in data. The interpolation/extrapolations points are not included in the evaluation of the performance of the methods.

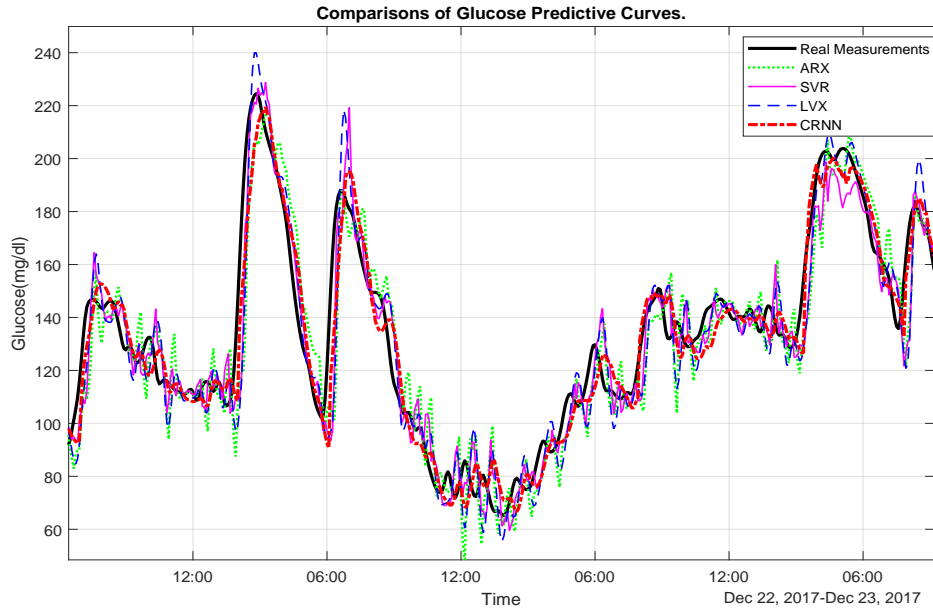


Fig. 5. One-day period prediction results for virtual adult 4. The solid black line, dotted green line, solid magenta line, dashed blue line, dash-dotted red line indicate the simulated glucose measurements, the prediction results of the 3rd order ARX method, the prediction results of the SVR method, the prediction results of the LVX algorithm, the prediction results of the CRNN method, respectively.

TABLE II
RMSE AND MARD COMPARISON OF DIFFERENT PREDICTION METHODS
FOR 10 REAL ADULT DIABETIC SUBJECTS

PH	Metric	CRNN	NNPG	SVR	LVX	ARX	
		Overall					
30	RMSE (mg/dL)	21.07 ±2.35	23.14 ±2.99	22.00 ±2.83	21.51 ±2.44	21.56 ±2.53	
	MARD (%)	11.61 ±2.18	13.42 ±2.35	13.54 ±2.88	10.93 ±1.87	11.00 ±1.81	
	Hyperglycaemia						
	MCC	0.79 ±0.04	0.75 ±0.04	0.79 ±0.05	0.79 ±0.04	0.77 ±0.04	
	Hypoglycaemia						
	MCC	0.51 ±0.2	0.12 [‡] ±0.12	0.11 [‡] ±0.08	0.55 ±0.17	0.53 ±0.15	
	Effective Prediction Horizon						
	Time (min)	19.3 ±3.1	12.8 [†] ±2.9	18.6 ±2.8	14.5 ±3.4	12.0 [*] ±3.0	
	60	Overall					
		RMSE (mg/dL)	33.27 ±4.79	36.05 [‡] ±4.85	34.35 [†] ±4.55	37.46 [‡] ±5.04	36.97 [‡] ±4.75
MARD (%)		19.01 ±4.46	21.98 [‡] ±4.87	20.65 ±3.92	19.69 [‡] ±3.70	19.65 [‡] ±3.55	
Hyperglycaemia							
MCC		0.72 ±0.05	0.66 [*] ±0.09	0.74 ±0.07	0.76 ±0.05	0.71 ±0.05	
Hypoglycaemia							
MCC		0.40 ±0.13	0.01 [‡] ±0.00	0.06 [‡] ±0.08	0.56 [*] ±0.14	0.51 ±0.15	
Effective Prediction Horizon							
Time (min)		29.3 ±9.4	18.3 [‡] ±4.9	28.4 ±5.2	19.9 [*] ±5.1	13.6 [‡] ±3.7	

* p -value ≤ 0.05 † p -value ≤ 0.01 ‡ p -value ≤ 0.005

Table II shows the RMSE and MARD of the performance of the algorithms for the 10 cases of real data. Contrary to the relative performance of the methods in the in-silico dataset, the evaluation of the methods is mixed. The CRNN

maintains the best results for RMSE and MARD over a 30 minute prediction horizon baseline methods. However, the ARX and LVX models show improved performance in terms of MARD relative to the CRNN. In addition, the LVX shows marginally better performance over CRNN in predicting adverse glycaemic events. The time delay in predicting these results shows that CRNN exhibits the best performance with the smallest lag.

Over a long-term prediction horizon, the CRNN provides the best performance for prediction of glucose level and with the least lag of the evaluated methods. SVR is able to perform close to the CRNN in terms of effective prediction horizon. However, the better prediction of hyperglycaemic events is contrasted with very poor prediction of hypoglycaemia. The results for hypoglycaemia prediction, equivalent to random guessing, suggest that 60 minutes represents the limit of meaningful hypoglycaemia prediction for SVR and NNPG given these inputs. Further improvement may require the inclusion of engineered features. Although LVX exhibits superior performance in predicting adverse glycaemic events, it should be noted that the user would have considerably less time (-9 mins) to take action. As seen in Fig. 6, the CRNN and LVX both achieve good predictive curves compared to the ground truth measurements. Specifically, at the inflection periods during peaks and troughs, the LVX tends to have higher and lower predictions, respectively. The CRNN follows the trend at both local and global peak points closely, which increases its overall accuracy.

To understand the effect of each network component, we generate networks with different components and evaluate their performances. The results are shown in Table III. It shows that full CRNN achieves the best performance, and both CNN and LSTM component contribute to the final result. In addition, we investigate the influence of different lengths

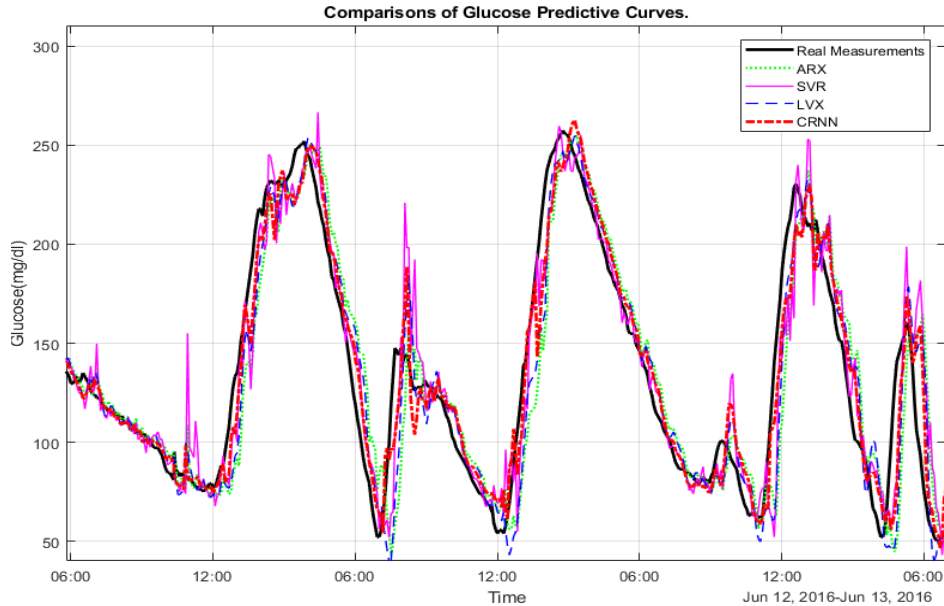


Fig. 6. One-day period prediction results for clinical adult 17. The solid black line, dotted green line, solid magenta line, dashed blue line, dash-dotted red line indicate the real glucose measurements, the prediction results of ARX, SVR, LVX, and the CRNN algorithm, respectively.

of training set. The results are in Table IV. Using 1 month training data, the RMSE of CRNN can achieve 22.28 ± 2.67 (30) and 35.56 ± 4.55 (60). This can be slightly improved if longer training data are exploited. It shows that collecting more training data can increase the predictive accuracy.

TABLE III
AN ABLATION STUDY SHOWING THE EFFECT OF EACH STAGE ON CRNN PERFORMANCE

Model	RMSE	
	30 min	60 min
CRNN	21.07 ± 2.35	33.27 ± 4.79
CRNN w/o CNN	22.16 ± 4.39	36.28 ± 7.14
CRNN w/o LSTM	21.50 ± 2.62	36.01 ± 6.41

TABLE IV
A TABLE SHOWING THE PERFORMANCE WITH DIFFERENT PERIODS OF TRAINING DATA

Training Data	RMSE	
	30 min	60 min
3 months	21.07 ± 2.35	33.27 ± 4.79
2 months	22.07 ± 2.84	35.12 ± 4.69
1 month	22.28 ± 2.67	35.56 ± 4.55

V. DISCUSSION

A. Performance in Simulated and Clinical Data

In this paper, both *in silico* and clinical dataset are verified. The *in silico* dataset is for test. The clinical dataset, as real data collected from clinical trials, are more practical and significant if people want to compare the performances of different methods. In the previous section we noted a discrepancy in the performance of the proposed algorithm and baseline algorithms in simulated cases and the real patient cases. Previous tests have also indicated that the performance

in real subjects is much less satisfactory comparing to virtual subjects. In our opinion, the drop in performance can be primarily attributed to the increased complexity of real data generated from a patient relative to the simulated data generated from a physiological model. In addition the gaps in data and method of interpolation/extrapolation may contribute to the further reduction in performance. Relative to the baseline algorithms, the CRNN is better at capturing the features since deep learning affords a better capacity at learning optimal representations of features. This would explain the relatively lower variance in metrics for the performance of the CRNN in different cases relative to baseline models.

B. Results Comparisons

We achieved a mean RMSE = 9.38mg/dL *in silico* using the proposed method, and it is the best amongst other algorithms, including SVR, LVX and 3rd order ARX. In addition, we want to compare our algorithm with other approaches in the literature. Using dataset generated from simulators, our algorithm is better than the results of RMSE = 18.78mg/dL [34] and RMSE = 13.65mg/dL in [35]. For several other works, it is difficult to evaluate the RMSE through direct comparison due to the unavailability of codes, parameters of the models, and the benchmark datasets. However, we may compare the results with widely used methods as benchmarks, such as SVR or NNPG. For instance, for PH = 30 min as shown in Table 3 [16], the algorithm is 0.1 mg/dL better than the result of SVR in terms of RMSE on the real dataset; our algorithm is 0.9 mg/dL better than the SVR in terms of RMSE on the real dataset. In [15], for PH = 30 min their RMSEs are 1.3 better than NNPG for the simulated data and 0.2 mg/dL better than NNPG for the real datasets. Our RMSEs are 3.5 mg/dL better than NNPG for the simulated data and 2.1 mg/dL better for the real datasets. As far as we know,

the proposed algorithm achieves a performance state-of-the-art accuracy with regard to RMSE. To build a fair comparison, we provide all benchmark models the same input, including CGM data, meal and insulin. For the conventional NNPG, it only uses CGM measurements. Thus in the comparison we incorporate meal and insulin in the input as well to generate an enhanced NNPG.

C. Application on resource-constrained mobile platforms

CRNN is a personalised algorithm for different diabetic subjects. Firstly, it is data driven and personalised. Secondly, the model can be continuously updated as more data is available. In details, the model is saved as a trained neural network. We use the sequential model with Tensorflow backend to train the neural network, and the result can be saved as a small file. This file can be compiled as a “.tflite” or a “.pb” file for the app on mobiles, by using a Tensorflow Lite converter. The model file can be updated continuously at the cloud. The app may demonstrate the predictive glycaemic curve on screen. A demonstration on the Android system is shown in Fig. 7 In addition, we also found that the execution time of the model is 6ms on a Android phone (LG Nexus5 with Processor: 2.26GHz quad-core, RAM:2GB) and 780ms on a laptop (MacPro with Processor: 3.1GHz Intel Core i5, RAM:8GB). The reasons might be in the quantisation of weights and biases (e.g. 8 bit integer vs. 32 bit floating point), thus leading to a faster computation.

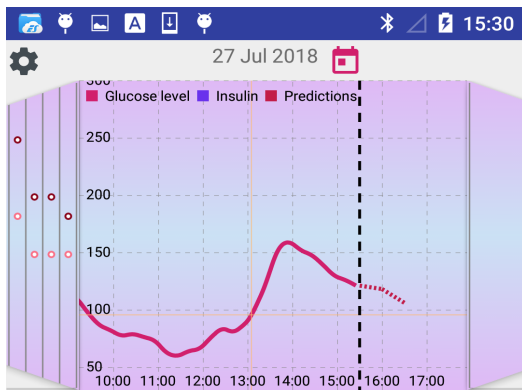


Fig. 7. An illustration of the glucose level shown in an app interface on an Android system, where the red curve is the historic blood glucose, black dash line is the current time, and the red dot curve is the prediction provided by the model.

D. Limitations

Though CRNN has achieved very good accuracy in prediction, some challenges remain. Notably the performance in predicting hypoglycaemia degrades much faster than the performance in predicting hyperglycaemia as the prediction horizon increases. This can relate to the intervention with unaccounted fast acting (< 15 mins) carbohydrates to prevent onset of hypoglycaemia or aerobic exercise which can accelerate onset of hypoglycaemia. Over farther prediction horizons, future events may need to be accounted for to improve the performance. In addition, meal/bolus rules supported by

physiological models might be added to the model. Based on the CRNN approach proposed in this paper, it is possible to develop a hybrid method, which may have the advantages of both conventional and deep learning algorithms.

VI. CONCLUSION

In this paper a convolutional recurrent neural network was proposed as an effective method for BG prediction. The architecture includes a multi-layer CNN followed by a modified RNN, where the CNN could capture the features or patterns of the multi-dimensional time series. The modified RNN is capable of analyzing the previous sequential data and providing the predictive BG. The method trains models for each diabetic subject using their own data. After obtaining the trained neural network, it could be applied locally or on portable devices. The proposed CRNN method showed superior performance in forecasting BG levels (RMSE and MARD) in the *in silico* and clinical experiments. lag.

VII. ACKNOWLEDGEMENTS

The authors thank EPSRC, ARISES project for support and providing the clinical data. We would also like to thank Prof. R. Spence, T. Zhu and C. Demasson’s for the contribution to the mobile app interface design.

VIII. APPENDIX

TABLE V
A TABLE DETAILING THE SIZE AND DIMENSIONS OF LAYERS IN CRNN

Layer Description (layer)	Output Dimensions	No. of Parameters
Convolutional Layers (Batch×Steps×Channels)		
(1) 1×4 conv	128(1) × 24 × 8	104
max_pooling, size 2	128(1) × 12 × 8	–
(2) 1×4 conv	128(1) × 12 × 16	528
max_pooling, size 2	128(1) × 6 × 16	–
(3) 1×4 conv	128(1) × 6 × 32	2080
max_pooling	128(1) × 3 × 32	–
Recurrent Layer (Batch×Cells)		
(4) lstm	128(1) × 64	24832
Dense Layers (Batch×Units)		
(5) dense	128(1) × 256	16640
(6) dense	128(1) × 32	8224
(7) dense	128(1) × 1	33

REFERENCES

- [1] N. D. D. Group, “Classification and diagnosis of diabetes mellitus and other categories of glucose intolerance,” *Diabetes*, vol. 28, no. 12, pp. 1039–1057, 1979.
- [2] A. Facchinetti, S. Favero, G. Sparacino, and C. Cobelli, “An online failure detection method of the glucose sensor-insulin pump system: Improved overnight safety of type-1 diabetic subjects,” *IEEE Transactions on Biomedical Engineering*, vol. 60, no. 2, pp. 406–416, Feb. 2013.
- [3] S. Zavitsanou, A. Mantalaris, M. C. Georgiadis, and E. N. Pistikopoulos, “In silico closed-loop control validation studies for optimal insulin delivery in type 1 diabetes,” *IEEE Transactions on Biomedical Engineering*, vol. 62, no. 10, pp. 2369–2378, Oct. 2015.
- [4] M. Vettoretti, A. Facchinetti, G. Sparacino, and C. Cobelli, “Type 1 diabetes patient decision simulator for in silico testing safety and effectiveness of insulin treatments,” *IEEE Transactions on Biomedical Engineering*, pp. 1–1, 2018.

- [5] M. M. Ahmadi and G. A. Jullien, "A wireless-implantable microsystem for continuous blood glucose monitoring," *IEEE Transactions on Biomedical Circuits and Systems*, vol. 3, no. 3, pp. 169–180, Jun. 2009.
- [6] A. Facchinetti, "Continuous glucose monitoring sensors: Past, present and future algorithmic challenges," *Sensors*, vol. 16, no. 12, 2016.
- [7] S. Oviedo, J. Vehi, R. Calm, and J. Armengol, "A review of personalized blood glucose prediction strategies for T1DM patients," *International Journal for Numerical Methods in Biomedical Engineering*, vol. 33, no. 6, p. 2833, 2017.
- [8] P. Pesi, P. Herrero, M. Reddy, M. Xenou, N. Oliver, D. Johnston, C. Toumazou, and P. Georgiou, "An advanced bolus calculator for type 1 diabetes: System architecture and usability results," *IEEE Journal of Biomedical and Health Informatics*, vol. 20, no. 1, pp. 11–17, Jan 2016.
- [9] A. G. Karegowda, M. Jayaram, and A. Manjunath, "Cascading k-means clustering and k-nearest neighbor classifier for categorization of diabetic patients," *International Journal of Engineering and Advanced Technology*, vol. 1, no. 3, pp. 2249 – 8958, 2012.
- [10] E. I. Georga, V. C. Protopappas, D. Ardigo, M. Marina, I. Zavaroni, D. Polyzos, and D. I. Fotiadis, "Multivariate prediction of subcutaneous glucose concentration in type 1 diabetes patients based on support vector regression," *IEEE Journal of Biomedical and Health Informatics*, vol. 17, no. 1, pp. 71–81, Jan 2013.
- [11] K. Yan and D. Zhang, "Blood glucose prediction by breath analysis system with feature selection and model fusion," in *36th Annual International Conference of the IEEE Engineering in Medicine and Biology Society*, Aug. 2014, pp. 6406–6409.
- [12] H. Abdi and L. J. Williams, "Principal component analysis," *Wiley Interdisciplinary Reviews: Computational Statistics*, vol. 2, no. 4, pp. 433–459, 2010.
- [13] K. Polat, S. Gunes, and A. Arslan, "A cascade learning system for classification of diabetes disease: Generalized discriminant analysis and least square support vector machine," *Expert Systems with Applications*, vol. 34, no. 1, pp. 482 – 487, 2008.
- [14] C. Pérez-Gandía, A. Facchinetti, G. Sparacino, C. Cobelli, E. Gómez, M. Rigla, A. de Leiva, and M. Hernando, "Artificial neural network algorithm for online glucose prediction from continuous glucose monitoring," *Diabetes technology & therapeutics*, vol. 12, no. 1, pp. 81–88, 2010.
- [15] C. Zecchin, A. Facchinetti, G. Sparacino, G. D. Nicolao, and C. Cobelli, "Neural network incorporating meal information improves accuracy of short-time prediction of glucose concentration," *IEEE Transactions on Biomedical Engineering*, vol. 59, no. 6, pp. 1550–1560, Jun. 2012.
- [16] K. Plis, R. Bunescu, C. Marling, J. Shubrook, and F. Schwartz, "A machine learning approach to predicting blood glucose levels for diabetes management," in *Modern Artificial Intelligence for Health Analytics Papers from the AAAI-14*.
- [17] M. v. d. W. H.N. Mhaskar, S.V. Pereverzyev, "A deep learning approach to diabetic blood glucose prediction," <https://arxiv.org/abs/1707.05828>, 2017.
- [18] C. Marling and R. Bunescu, "The OhioT1DM dataset for blood glucose level prediction," in *The 3rd International Workshop on Knowledge Discovery in Healthcare Data*, Stockholm, Sweden, July 2018, CEUR proceedings in press, available at <http://smarthealth.cs.ohio.edu/bglp/OhioT1DM-dataset-paper.pdf>.
- [19] Y. Jia, E. Shelhamer, J. Donahue, S. Karayev, J. Long, R. Girshick, S. Guadarrama, and T. Darrell, "Caffe: Convolutional architecture for fast feature embedding," in *Proceedings of the 22Nd ACM International Conference on Multimedia*, ser. MM '14. New York, NY, USA: ACM, 2014, pp. 675–678.
- [20] G. Litjens, C. I. Sanchez, N. Timofeeva, M. Hermsen, I. Nagtegaal, I. Kovacs, C. H. van de Kaa, P. Bult, B. van Ginneken, and J. van der Laak, "Deep learning as a tool for increased accuracy and efficiency of histopathological diagnosis," *Scientific Reports*, vol. 6, p. 26286, May 2016.
- [21] R. Miotto, F. Wang, S. Wang, X. Jiang, and J. T. Dudley, "Deep learning for healthcare: review, opportunities and challenges," *Briefings in Bioinformatics*, vol. 19, no. 6, pp. 1236–1246, 05 2017.
- [22] T. Zhu, K. Li, P. Herrero, J. Chen, and P. Georgiou, "A deep learning algorithm for personalized blood glucose prediction," in *The 3rd International Workshop on Knowledge Discovery in Healthcare Data, IJCAI-ECAI 2018*, Stockholm, Sweden, July 2018.
- [23] Y. Bengio, "Deep learning of representations: Looking forward," in *Statistical Language and Speech Processing*. Berlin, Heidelberg: Springer Berlin Heidelberg, 2013, pp. 1–37.
- [24] J. Schmidhuber, "Deep learning in neural networks: An overview," *Neural Networks*, vol. 61, pp. 85 – 117, 2015.
- [25] K. Li, A. Javer, E. Keaveny, and A. Brown, "Recurrent neural networks with interpretable cells predict and classify worm behaviour," in *Workshop on Worm's Neural Information Processing (WNIP) in NIPS*, CA, USA, 2017.
- [26] Q. Zhang, Y. N. Wu, and S.-C. Zhu, "Interpretable convolutional neural networks," in *The IEEE Conference on Computer Vision and Pattern Recognition (CVPR)*, Jun. 2018, pp. 8827–8836.
- [27] I. Goodfellow, Y. Bengio, and A. Courville, *Deep Learning*. The MIT Press, 2016.
- [28] M. Abadi, A. Agarwal, P. Barham, E. Brevdo, Z. Chen, C. Citro, G. S. Corrado, A. Davis, J. Dean, M. Devin, S. Ghemawat, I. Goodfellow, A. Harp, G. Irving, M. Isard, Y. Jia, R. Jozefowicz, L. Kaiser, M. Kudlur, J. Levenberg, D. Mané, R. Monga, S. Moore, D. Murray, C. Olah, M. Schuster, J. Shlens, B. Steiner, I. Sutskever, K. Talwar, P. Tucker, V. Vanhoucke, V. Vasudevan, F. Viégas, O. Vinyals, P. Warden, M. Watteberg, M. Wicke, Y. Yu, and X. Zheng, "TensorFlow: Large-scale machine learning on heterogeneous systems," 2015, software available from tensorflow.org.
- [29] C. Zhao, E. Dassau, L. Jovanovic, H. C. Zisser, I. Francis J. Doyle, and D. E. Seborg, "Predicting subcutaneous glucose concentration using a latent-variable-based statistical method for type 1 diabetes mellitus," *Journal of Diabetes Science and Technology*, vol. 6, no. 3, pp. 617–633, 2012, pMID: 22768893.
- [30] D. A. Finan, F. J. Doyle III, C. C. Palerm, W. C. Bevier, H. C. Zisser, L. Jovanović, and D. E. Seborg, "Experimental evaluation of a recursive model identification technique for type 1 diabetes," *Journal of diabetes science and technology*, vol. 3, no. 5, pp. 1192–1202, 2009.
- [31] "The uva/padova type 1 diabetes simulator," *Journal of Diabetes Sci Technol.*, vol. 8, no. 1.
- [32] P. Herrero, J. Bondia, O. Adewuyi, P. Pesi, M. El-Sharkawy, M. Reddy, C. Toumazou, N. Oliver, and P. Georgiou, "Enhancing automatic closed-loop glucose control in type 1 diabetes with an adaptive meal bolus calculator—in silico evaluation under intra-day variability," *Computer Methods and Programs in Biomedicine*, vol. 146, pp. 125–131, 2017.
- [33] M. Reddy, P. Pesi, M. Xenou, C. Toumazou, D. Johnston, P. Georgiou, P. Herrero, and N. Oliver, "Clinical safety and feasibility of the advanced bolus calculator for type 1 diabetes based on case-based reasoning: A 6-week nonrandomized single-arm pilot study," *Diabetes Technology & Therapeutics*, vol. 18, no. 8, pp. 487–493, 2016, pMID: 27196358.
- [34] G. Sparacino, F. Zanderigo, S. Corazza, A. Maran, A. Facchinetti, and C. Cobelli, "Glucose concentration can be predicted ahead in time from continuous glucose monitoring sensor time-series," *IEEE Transactions on Biomedical Engineering*, vol. 54, no. 5, pp. 931–937, May 2007.
- [35] S. G. Mougialakou, A. Prountzou, D. Iliopoulou, K. S. Nikita, A. Vazeou, and C. S. Bartsocas, "Neural network based glucose - insulin metabolism models for children with type 1 diabetes," in *2006 International Conference of the IEEE Engineering in Medicine and Biology Society*, Aug. 2006, pp. 3545–3548.
- [36] R. Atanassov, P. Bose, M. Couture, A. Maheshwari, P. Morin, M. Paquette, M. Smid, and S. Wuhrer, "Algorithms for optimal outlier removal," *Journal of Discrete Algorithms*, vol. 7, no. 2, pp. 239 – 248, 2009, selected papers from the 2nd Algorithms and Complexity in Durham Workshop ACID 2006.
- [37] H. Shum, K. Ikeuchi, and R. Reddy, *Principal Component Analysis with Missing Data and Its Application to Polyhedral Object Modeling*. Boston, MA: Springer US, 2001, pp. 3–39.
- [38] D. Li, J. Deogun, W. Spaulding, and B. Shuart, "Towards missing data imputation: A study of fuzzy k-means clustering method," in *Rough Sets and Current Trends in Computing*, S. Tsumoto, R. Słowiński, J. Komorowski, and J. W. Grzymała-Busse, Eds. Berlin, Heidelberg: Springer Berlin Heidelberg, 2004, pp. 573–579.
- [39] L. Lekha and S. M, "Real-time non-invasive detection and classification of diabetes using modified convolution neural network," *IEEE Journal of Biomedical and Health Informatics*, pp. 1–1, 2018.
- [40] S. Hochreiter and J. Schmidhuber, "Long Short-Term Memory," *Neural Computation*, vol. 9, no. 8, pp. 1735–1780, 1997.
- [41] A. Graves, A. R. Mohamed, and G. Hinton, "Speech recognition with deep recurrent neural networks," in *IEEE Int. Conf. on Acou., Spe. and Sig. Proc.*, 2013, p. 6645.
- [42] N. Srivastava, G. E. Hinton, A. Krizhevsky, I. Sutskever, and R. Salakhutdinov, "Dropout: a simple way to prevent neural networks from overfitting," *Journal of Machine Learning Research*, vol. 15, no. 1, pp. 1929–1958, 2014.
- [43] S. Ruder, "An overview of gradient descent optimization algorithms," 2016. [Online]. Available: [preprintarXiv:1609.04747](https://arxiv.org/abs/1609.04747)
- [44] International Hypoglycaemia Study Group, "Glucose Concentrations of Less Than 3.0 mmol/L (54 mg/dL) Should Be Reported in Clinical Trials: A Joint Position Statement of the American Diabetes Association and the European Association for the Study of Diabetes: Table 1," *Diabetes Care*, vol. 40, no. 1, pp. 155–157, Jan. 2017.